

Profile measurement using rotated digital image correlation

J. R. PARRA MICHEL^{a,*}, DAVID ASael GUTIÉRREZ HERNÁNDEZ^{a,b}, MARCO A. ESCOBAR^c, ALMA CAMACHO-PÉREZ^a, RAFAEL MARTÍNEZ-PELÁEZ^a

^a*Escuela de Ingenierías. Universidad De La Salle Bajío, Av. Universidad 602, Col. Lomas del Campestre, León, Guanajuato, México.*

^b*Tecnológico Nacional de México. Instituto Tecnológico de León. División de Estudios de Posgrado e Investigación. Avenida Tecnológico s/n, Industrial Julián de Obregón, 37290 León, Guanajuato, México.*

^c*Universidad De La Salle Bajío campus Salamanca. Libramiento a Morelia km 7.5 Poblado de San Juan de Razos, 36700, Salamanca, Gto., México.*

An optical technique based on a rotated digital image correlation for measuring the full topographic field profile of a surface is proposed. The mathematical models, and possible sources of errors during measurements, are presented and properly analyzed. A comparison between measured results for regular and irregular surfaces, and their respective physical models, is shown. Experimental resolutions of down to 10 microns can be obtained.

(Received September 7, 2016; accepted April 6, 2017)

Keywords: Phase Retrieval, Fringe Projection, Profilometry, Digital Image Correlation

1. Introduction

There are several optical techniques for measuring topographic profiles on surfaces. Some of those techniques are complicated, and require the simultaneous use of several instruments [1]. One of the most widespread techniques is the projection of structured light, this technique consists on a light projection system and a well-defined constant fringe pattern [2]. In the fringe projection technique, the topographic profile is associated with the phase change on the observed pattern. Another technique, the Moiré pattern [3] is very useful for measuring the topographic profile of the surface. In the Moiré pattern, it is common to use a Ronchi grating, and to illuminate both the grating and the surfaces with uniform light. A camera observes simultaneously the Ronchi grid and the Ronchi grid shadow projected on the object. The superposition of both projections forms a pattern that recreates the Moiré-effect curves, and then the observed shadows are associated with surface topography.

Another optical technique for measuring topographic profiles is the electronic speckle pattern interferometry (ESPI) in which either divergent or collimated laser illumination is required over the surface to be measured [4]. In ESPI, it is also necessary to account for the phase shift of the associated topographic profile or use the Fourier technique to get the optical phase.

Stereoscopic Photogrammetry is a widely used measurement technique for topographic profiles. This technique involves taking two or more pictures of the surface from different known coordinates. Subsequently the position of several recognizable points on the images are located to associate these measurements with the

topographic profile of the surface. In this technique the digital image correlation can be applied in 3-D [5], by simultaneously using two CCD cameras located in different positions for recording the information associated with the surface.

In combination with other techniques, digital image correlation (DIC) has been used in various methods for determining both the deformation and the topographic profile of surfaces. For example, DIC has been used in conjunction with a spot pattern projection in order to obtain a topographical surface profile [6,7]. Also, fringe projection together with DIC have been used for measuring 3-D deformations [8]. Bear in mind that all these techniques require the use of multiple instruments simultaneously, and this can increase measurement uncertainty due to the law of propagation of uncertainty [9,10].

In order to simplify the optical arrangements, and to avoid using multiple instruments simultaneously, we propose a technique based on digital image correlation that uses only a digital camera and a rotation base. The proposed technique allows measurements of the topographic surface profile by observing the shift on the speckle pattern at the surface after a small angle rotation of the surface takes place.

2. Theoretical background

To facilitate correlation, images are divided into small regions called Region of Interest (ROI). Generally, the ROIs size are determined manually with a square dimension of $(2m+1) \times (2m+1)$ pixels centred at the point

$P(x_0, y_0)$, as it can be seen in Fig. 1. However, it has been observed that the optimum size of the ROI is dependent on the quality and the size of speckle [13].

Small high-contrast speckles allow to achieve a smaller ROI size and therefore better resolution measurements.

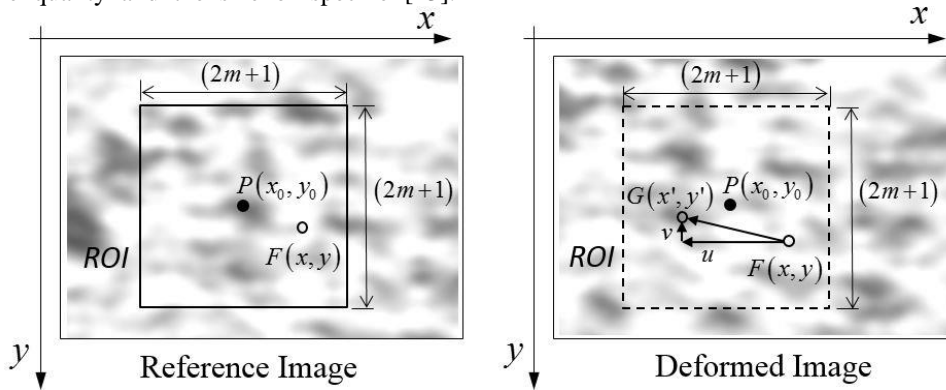


Fig. 1. Correlation of two images. In a General case, it is possible to observe the displacement u and v from the speckle pattern in the ROI of the deformed image with respect to the reference image. x and y axis are the dimensions of the image given in pixels

In strain measurements, full field resolution is obtained by comparing the distribution of speckles within the ROI of images obtained before and after deformation. It is also possible to evaluate the deformation process with the acquisition of several images at constant intervals. Generally, the initial images observe deformation-free surface, and they are used as reference. Subsequent images are correlated with the initial ones in order to analyse the position and displacement of the speckles during deformation. The displacement of the speckles is directly associated with the deformation of the observed surface.

DIC is a procedure that compares the ROI between different images. Between each comparison a correlation function is established as:

$$S\left(x, y, u, v, \frac{\partial u}{\partial x}, \frac{\partial u}{\partial y}, \frac{\partial v}{\partial x}, \frac{\partial v}{\partial y}\right) = 1 - \{C.C.\} \quad (1)$$

With $\{C.C.\}$ taken as the normalized cross correlation, given by

$$\{C.C.\} = \frac{\sum_{i=-m}^m \sum_{j=-m}^m [F(x_i, y_j)G(x'_i, y'_j)]}{\sqrt{\sum_{i=-m}^m \sum_{j=-m}^m [F(x_i, y_j)]^2 \sum_{i=-m}^m \sum_{j=-m}^m G(x'_i, y'_j)^2}} \quad (2)$$

where $F(x_i, y_j)$ is the grayscale intensity at (x_i, y_j) of the reference image, and $G(x'_i, y'_j)$ is the grayscale intensity of the strained sample image at (x'_i, y'_j) . In literature it is possible to find several definitions for the $\{C.C.\}$, they can be divided into: cross correlation criteria [14], and sum of squared differences [15]. The relation between coordinates (x_i, y_j) and (x'_i, y'_j) is given by

$$x'_i = x_i + u + \Delta x \frac{\partial u}{\partial x} + \Delta y \frac{\partial u}{\partial y} \quad (3a)$$

$$y'_j = y_j + v + \Delta y \frac{\partial v}{\partial y} + \Delta x \frac{\partial v}{\partial x} \quad (3b)$$

The u, v terms are the displacements from the center of each ROI in the directions of x, y respectively. The derivate terms $\Delta x \frac{\partial u}{\partial x}, \Delta y \frac{\partial u}{\partial y}, \Delta y \frac{\partial v}{\partial y}$ and $\Delta x \frac{\partial v}{\partial x}$ are associated to normal and shear deformations observables in the ROI. Minimizing the correlation coefficients for each ROI, the best fit for the correlation function S is obtained, as seen in equation (2). Since the minimization is nonlinear, iterative methods (e.g. Newton-Raphson or Gauss-Seidel) are needed to be implemented for interpolating and finding the best fit parameters for the displacement function [16].

However, since the proposed method requires a rotation base with the axis parallel to y , then only displacements on the u direction can be observed, while v is invariant. As a result, this method only provides information of the surface that is parallel to the observation plane.

2.1. Obtaining the full field topographic profile

In figure 2 a schematic of the optical system for the proposed method is presented. The displacement in u direction will be observed on the xy plane of the optical system. A CCD camera is located on a point along the z axis in such a way that the center of the image is parallel to the center of the CCD detector. If a small in-plane rotation is applied to the S surface, a given point P is displaced by a distance d in to P' . The surface is not deformed at rotation, and consequently the camera will record the surface displacement u .

Using trigonometric identities, we see that $r(\theta)\Delta\theta = d$ and $u = d \cos(\theta + \Delta\theta/2)$. And then it is possible to find an expression for the u displacement as

$$\frac{u}{\Delta\theta} = r(\theta) \cos\left(\theta + \frac{\Delta\theta}{2}\right) \quad (4)$$

where $r(\theta)$ represent the topographic profile on the surface. As you can see $r(\theta)$ is modulated by a cosine function and a constant term which makes impossible to obtain measurements when $\theta \rightarrow \pm\pi/2$. In other hand, near the optical axis, when $\theta \rightarrow 0$, the equation (4) can be rewritten as

$$r(\theta) \approx \frac{u}{\Delta\theta} \quad (5)$$

It is necessary to establish a relation between θ and P on the surface of the object in order to solve the term

$\cos(\theta + \Delta\theta/2)$ in equation (4). In the same Fig. 2 we can establish the trigonometric relations:

$$x_0 = r(\theta) \sin(\theta) \quad (6)$$

$$z_0 = r(\theta) \cos(\theta) \quad (7)$$

By inserting equation (4) into (6), it is possible to find a relation between the angle θ and the x_0 coordinate of P in the form:

$$\frac{u}{\Delta\theta \cos\left(\theta + \frac{\Delta\theta}{2}\right)} = \frac{x_0}{\sin(\theta)}, \quad \left\{ -\frac{\pi}{2} < \theta < \frac{\pi}{2} \right\} \quad (8)$$

where u , x_0 , and $\Delta\theta$ are known values. The angle θ is calculated using a numerical method in order to find $r(\theta)$. The obtained values can be used in equation (7) to find the topographical profile of the surface S .

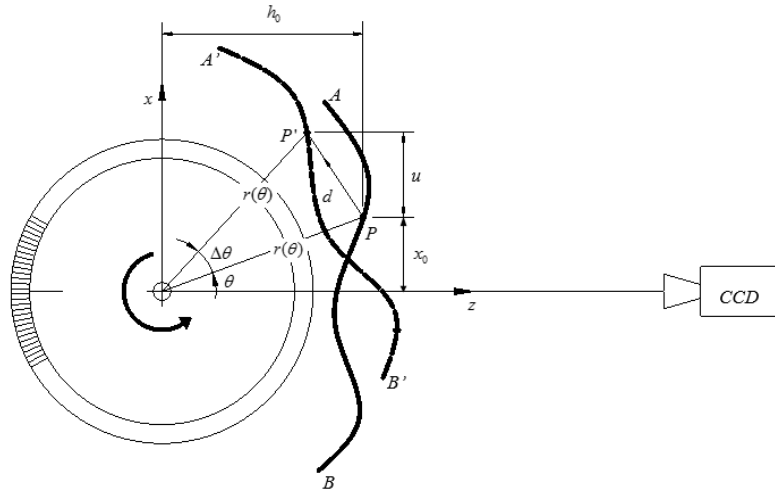


Fig. 2. Optical system schematic. The figure is not at scale

3. Numerical validation

In Fig. 3 a calculation is performed for a 90 mm side square plate, located at a distance of 11 mm from the center of rotation. The increment rotation is set to $\Delta\theta = 290.8 \times 10^{-6}$ rad (0.017°). The distance from the rotation center to each point of the plate is given by $r(\theta)$.

Using equation (4), we can find the rate of the displacement u of each point on the rotated plate. Notice that u can be obtained via DIC in case of real measurements. In figure 4a we can see that the plate center approaches to z_0 when θ goes to zero as is predicted in section 2.2.

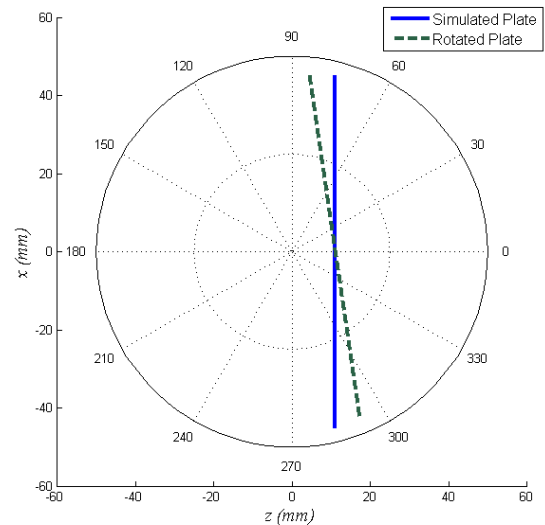
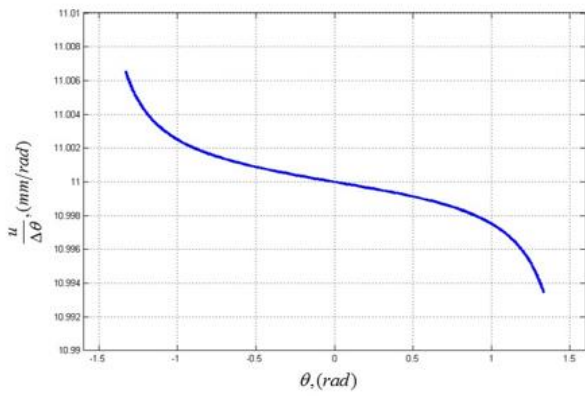
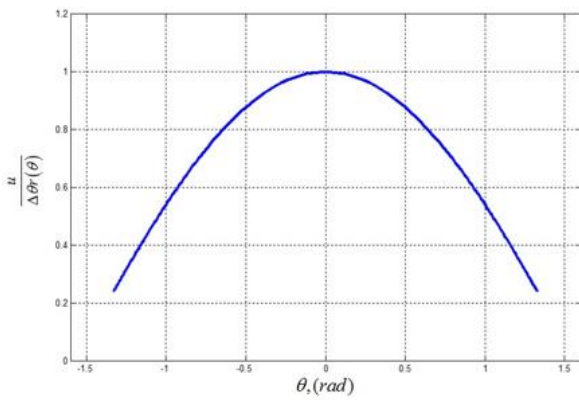


Fig. 3. Calculation of the plate at initial position and after rotation. The rotation $\Delta\theta$ was exaggerated for clarity propose.



a



b)

Fig. 4: a) Result obtained from equation (4), and b) Representation of $\cos\left(\theta + \frac{\Delta\theta}{2}\right)$. Notice that the results obtained come from a simulation, then $r(\theta)$ is known in advance

In Fig. 4b we can see the plot of the right part of equation (4) assuming a knowing $r(\theta)$. Fortunately, the function $\cos(\theta + \Delta\theta/2)$ can be obtained during the calibration of the optical system from equation (8) and (4) by means of numerical methods. In Fig. 5 a reconstruction of the plate is shown using section 2.2.

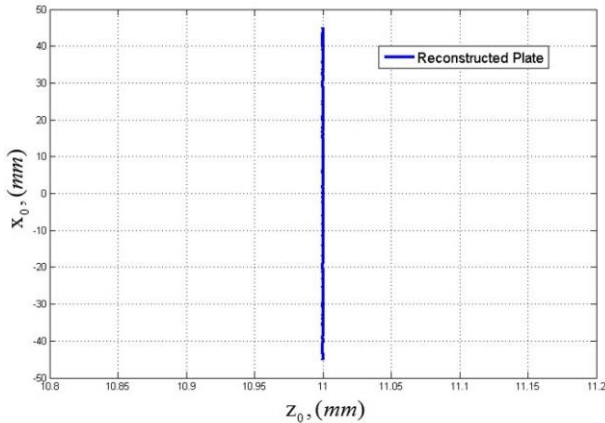
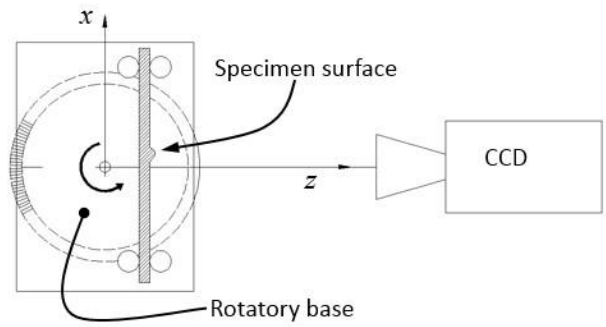


Fig. 5. Reconstructed plate

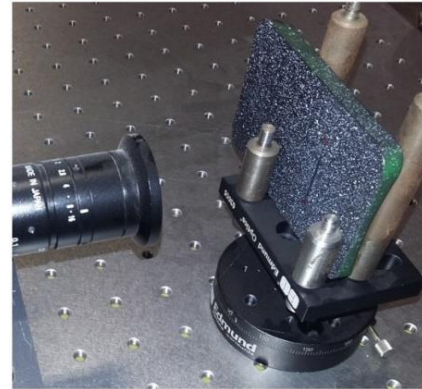
We can see that the presented method gives us a good reconstruction of the simulated plate. A complete superficial topography can be obtained repeating the same proses for each row in the set of data obtained for the u displacement generated by the DIC method.

4. Experimental results

A small metal plate painted with a random speckle pattern was used for an experimental test. The plate contains a 20 mm long defect at the center. A schematic of the optical system used is shown in Fig. 6.



a



b

Fig. 6. a) Theoretical optical setup, and b) experimental optical setup. Only a CCD camera, situated in front of the object, and a rotatory base for the object are needed for the experiment proposed in this work

A series of 60 images of the plate obtained with the CCD camera, each those images had a $\Delta\theta = 2.91 \times 10^{-6}$ rad rotation with respect to the previous one, this in order to observe a cumulative angle of $\Delta\theta_{acc} = 174.53 \times 10^{-3}$ rad. The displacement u is obtained from the digital correlation technique. The figure 7 shows the first and last image of the series. The analysis area is of $41.7\text{mm} \times 25.7\text{mm}$ (730×450 Pixel), and it is marked within the figure.

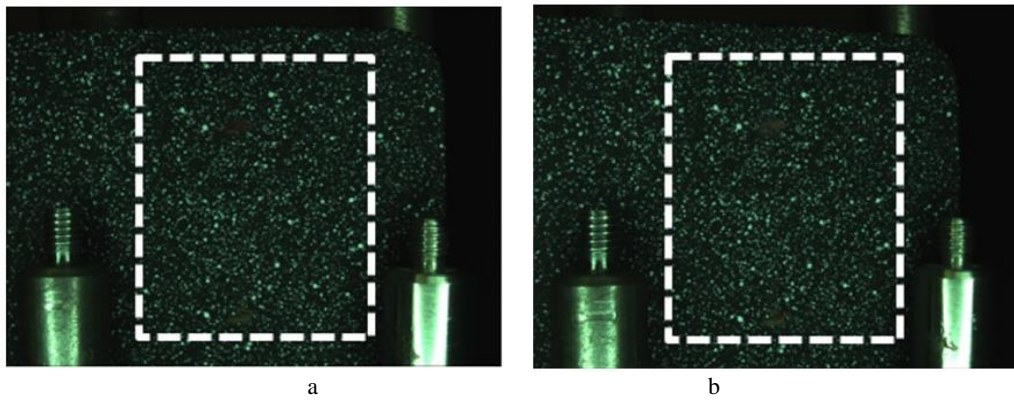


Fig. 7. a) First image at $\theta=0$ rad, and b) Last image at $\theta=0.175$ rad

The width (41.7 mm) and length (25.7 mm) of the analysed area are obtained by direct measurement. A resolution of $R = 0.0517$ mm/Pixel is calculated using pixel counting. The i -th image correlation was performed using the i -th and $(i+1)$ -th images. The displacement u_i accumulates to build up the total displacement u . Figure 8

shows an example of the evolution of displacement u for $\Delta\theta = 0.035, 0.087$ and 0.174 rad.

Using numerical methods, it is possible to find the angle θ from equation (8). After normalization, the term $\cos(\theta+\Delta\theta/2)$ is obtained and can be associated to $r(\theta)$. The result is shown in Fig. 9.

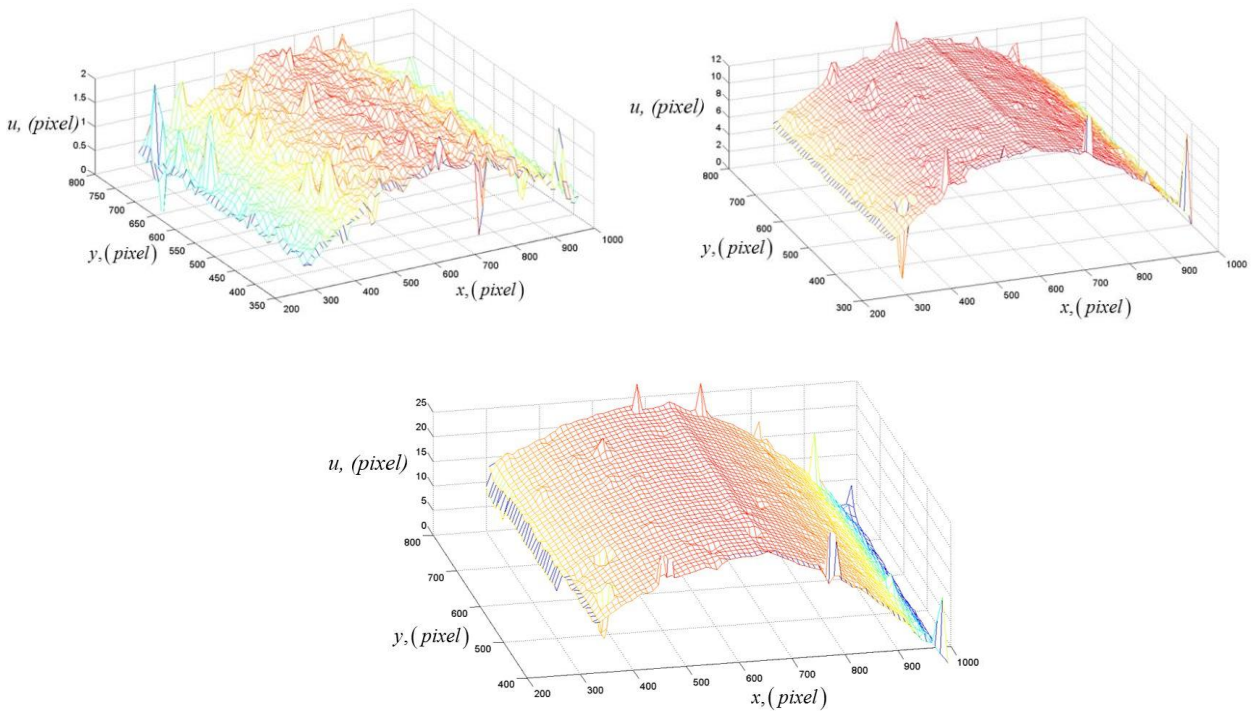


Fig. 8. Results of the displacements obtained by image correlation technique for three different angle increases of 0.035 rad, 0.087 rad and 0.172 rad respectively

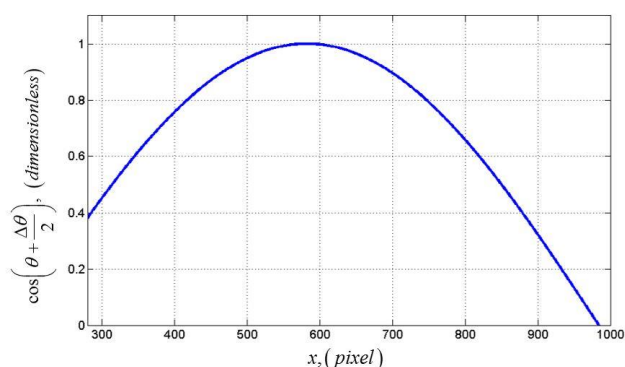


Fig. 9. Obtaining the cosine term for the images obtained

In Fig. 10, the result is shown for surface topography using equation (7) taking into consideration the resolution of the optical system.

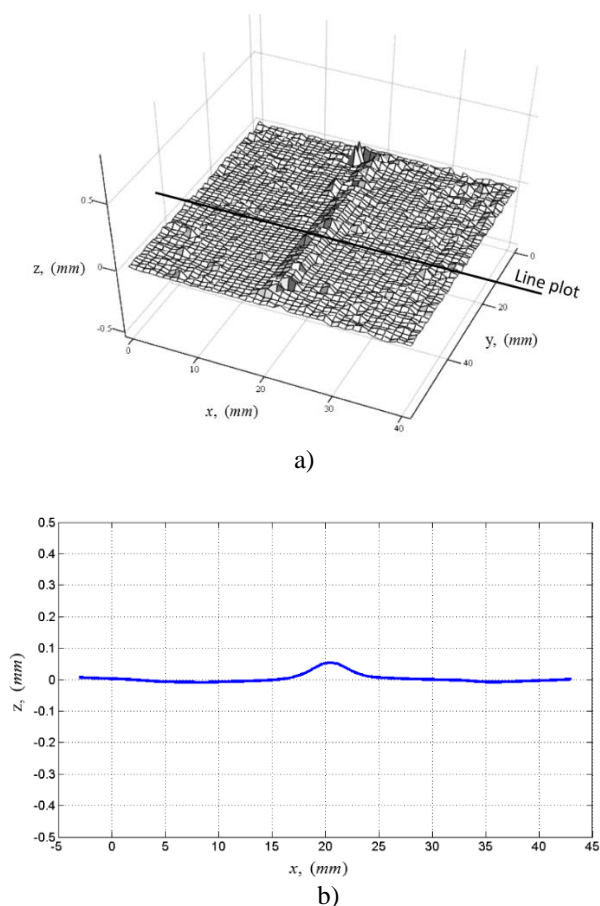


Fig. 10. a) topographic profile observed surface, b) measuring along the line marked.

Additionally, it is observed that the best measurements are obtained at the centre of the image studied and are degraded to the edges as a result of the cosine term of equation (4).

5. Conclusions

An optical technique based on a rotated digital image correlation for measuring the full topographic field profile of a surface was proposed. It is also important to obtain several images using a constant increasing in the rotation angle in order to obtain uniform displacements that can be associated with the sample shape. Making measurements at the edges of the sample might be difficult due to the cosine function. However, measurements at the center can be obtained with a resolution down to $50 \mu\text{m}$.

References

- [1] S. S. Gorthi, P. Rastogi, *Optics and Lasers in Engineering* **48**(2), 133 (2010).
- [2] R. Rodríguez-Vera, D. Vasquez, K. Genovese, J. Rayas, F. Mendoza-Santoyo, *Proc. SPIE 7155, Ninth International Symposium on Laser Metrology*, 71552A (2008).
- [3] C. A. Sciammarella, *Experimental Mechanics* **22**(11), 418 (1982).
- [4] J. Parra-Michel, A. Martínez, M. Anguiano-Morales, J. Rayas, *Measurement Science and Technology* **21**(4), 045303 (2010).
- [5] M. A. Sutton, J. J. Orteu, H. Schreier, *Image correlation for shape, motion and deformation measurements: basic concepts, theory and applications*: Springer Science & Business Media US, 1 (2009).
- [6] J. Brillaud, F. Lagattu, *Optik-International Journal for Light and Electron Optics* **117**(9), 411 (2006).
- [7] S. McNeill, M. Sutton, Z. Miao, J. Ma, *Experimental Mechanics* **37**(1), 13 (1997).
- [8] C. Quan, C. Tay, Y. Huang, *Optik-International Journal for Light and Electron Optics* **115**(4), 164 (2004).
- [9] P. Fornasini, *The uncertainty in physical measurements: an introduction to data analysis in the physics laboratory*: Springer Science & Business Media US (2008).
- [10] R. Willink, *Metrologia* **46**(3), 145 (2009).
- [11] B. Pan, K. Qian, H. Xie, A. Asundi, *Measurement Science and Technology* **20**(6), 062001 (2009).
- [12] H. Schreier, J.-J. Orteu, M. A. Sutton, *Image correlation for shape, motion and deformation measurements*: Springer US (2009).
- [13] B. Pan, H. Xie, Z. Wang, K. Qian, Z. Wang, *Optics express* **16**(10), 7037 (2008).
- [14] A. Giachetti, *Image and Vision Computing* **18**(3), 247 (2000).
- [15] W. Tong, *Strain* **41**(4), 167 (2005).
- [16] H. Bruck, S. McNeill, M. A. Sutton, W. Peters Iii, *Experimental Mechanics* **29**(3), 261 (1989).

*Corresponding author: jrparra@delasalle.edu.mx